THE JOURNAL OF PHYSICAL CHEMISTRY Letters

pubs.acs.org/JPCL

Water Transport through Ultrathin Graphene

Myung E. Suk and N. R. Aluru*

Department of Mechanical Science and Engineering, Beckman Institute for Advanced Science and Technology, University of Illinois at Urbana−Champaign, Urbana, Illinois 61801

ABSTRACT Graphene can be considered as an ideal membrane since its thickness is only one carbon diameter. In this study, using molecular dynamics simulations, we investigate water transport through a porous graphene membrane and compare the results with water transport through thin (less than 10 nm in thickness/length) carbon nanotube (CNT) membranes. For smaller diameter pores, where a single-file water structure is obtained, CNT membranes provide higher water flux compared to graphene membranes. For larger diameter pores, where the water structure is not single-file, graphene membranes provide higher water flux compared to CNT membranes. Furthermore, in thin CNT membranes, the water flux did not vary significantly with the thickness of the membrane. We explain the results through a detailed analysis considering pressure distribution, velocity profiles, and potential of mean force. This work opens up opportunities for graphene-based membranes in molecular sieving, water filtration, fuel cells, and so forth.

SECTION Surfactants, Membranes

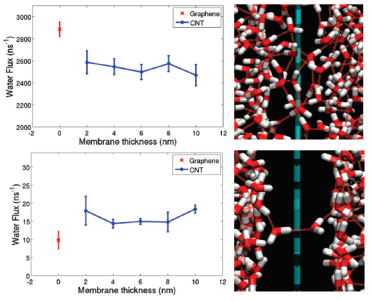

Because of the growing emphasis on water purification due to the water shortage problem,[1,2] development of novel and energy efficient membranes for water filtration is currently an area of immense research interest. In recent experimental work, novel membranes incorporating carbon nanotubes (CNT)[3−5] or biological water channels[6] have been investigated. Many theoretical[7−12] and experimental studies[4,5,13] have shown that nanotube-based membranes can be used for high molecular transport rate and solute rejection rate. Efforts were also made to decrease the thickness of the membrane to reduce pressure loss and increase the molecular transport rate. Porous silicon membranes as thin as 15 nm were fabricated by Striemer et al.[14] They observed more than an order of magnitude faster transport rate through these ultrathin membranes compared to thicker membranes made of silica−surfactant nanocomposite.[15]

A graphene monolayer[16] can be considered as the thinnest membrane reported so far, as its thickness is only one carbon atom in diameter. Because of the superior strength of graphene,[17,18] porous graphene is a potential membrane for molecular sieving or water filtration. Nanopores of various diameters can be realized in graphene via mono vacancies or multi vacancies.[19,20] Such vacancies can be generated by irradiation with an electron beam.[19,21] Ion selectivity and gas selectivity of porous graphene membrane have been theoretically studied by Sint et al.[22] and Jiang et al.,[23] respectively. However, transport of water through porous graphene membrane has not been reported in spite of its potential application in water purification. Our goal here is to investigate water transport through a porous graphene membrane, where the thickness approaches one atom diameter, and compare it to that of water transport through thin CNT membranes, which have already been reported as efficient membranes for filtration and other applications. We anticipate that this study will help identify the potential applications of graphene.

A graphene membrane with a nanopore was modeled as shown in Figure 1a. Various diameters of nanopores ranging from 0.75 to 2.75 nm were tested. Similarly, CNTs with diameters ranging from (10,0) CNT to (20,20) CNT were considered. CNT membranes were modeled with thicknesses or lengths varying from 2 to 10 nm and graphene slabs attached to them at the ends.[24] Edge dynamics,[20] partial charges,[23] or out-of-plane displacement[25] of graphene were excluded in this study to understand the effect of thickness of one-atom thin graphene membrane on water flow rate. Simulation set up with graphene membrane is as described in Figure 1b. Six nanometer water baths were included on each side of the membrane. Simulation set up with CNT membranes is the same as in Figure 1b except that the graphene membrane is replaced with a CNT membrane. Pressure-driven flow was simulated by applying a 100 MPa pressure drop across the pore (see Methods section for details), and water flux was calculated by counting the net amount of water molecules transported through the pore.

Figure 2 shows the comparison of water flux through graphene and CNT membranes. The thickness of the CNT membrane is varied from 2 to 10 nm in 2 nm increments.

Received Date: February 19, 2010
Accepted Date: April 26, 2010
Published on Web Date: April 30, 2010

DOI: 10.1021/jz100240r | *J. Phys. Chem. Lett.* **2010**, *1*, 1590–1594

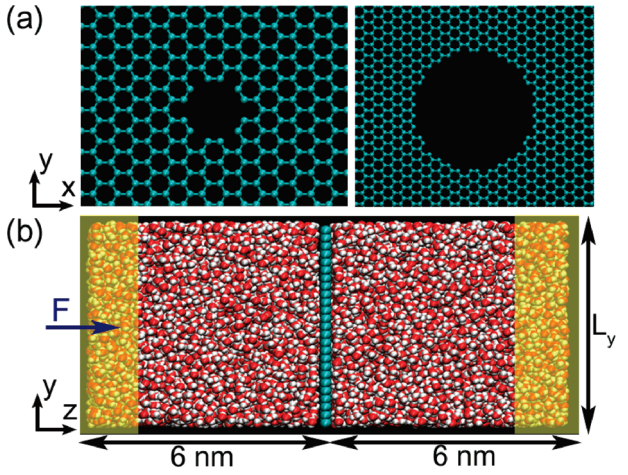

Figure 1. (a) Graphene membrane with a nanopore of diameter d_{avg} = 0.75 nm (left) and d_{avg} = 2.75 nm (right). (b) Simulation setup. Cyan color represents carbon atom, red color and white color represent the oxygen and hydrogen atoms of a water molecule, respectively. Two water reservoirs are attached to each side of the porous graphene membrane. $L_y = L_x$ = 4 nm when the pore diameter is 0.75 nm, and $L_y = L_x$ = 6 nm when the pore diameter is 2.75 nm. In the shaded region (Δz = 1 nm), external forces are applied on water molecules to create a pressure drop across the membrane.

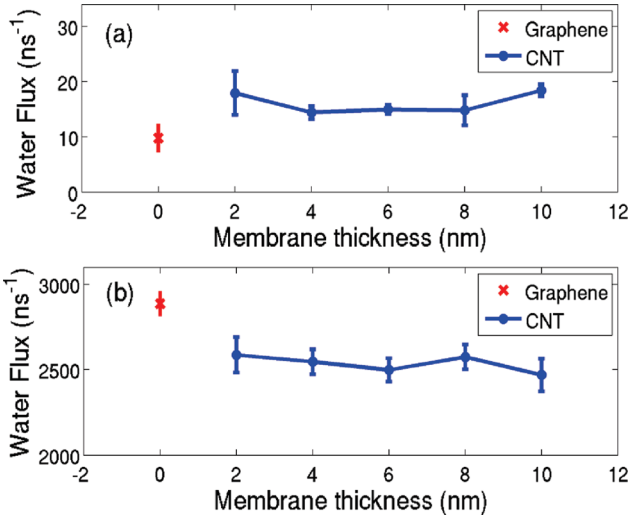

Figure 2. (a) Water flux through a (10,0) CNT with a diameter of 0.78 nm and through a graphene nanopore with a diameter of 0.75 nm. In both cases, single-file water structure is observed. (b) Water flux through a (20,20) CNT with a diameter of 2.71 nm and through a graphene nanopore with a diameter of 2.75 nm. Single-file water structure is not observed in this case.

In Figure 2a, water flux through the (10,0) CNT (diameter, d = 0.78 nm) is compared with the water flux through the 0.75 nm diameter pore graphene membrane. Similarly, in Figure 2b, water flux through the (20,20) CNT (d = 2.71 nm) is compared with that of the 2.75 nm diameter pore graphene membrane. Pore diameter and membrane thickness are calculated using the center-to-center distance of atoms. We note that, in Figure 2a,b, water flux through the CNT membrane did not change significantly with the membrane

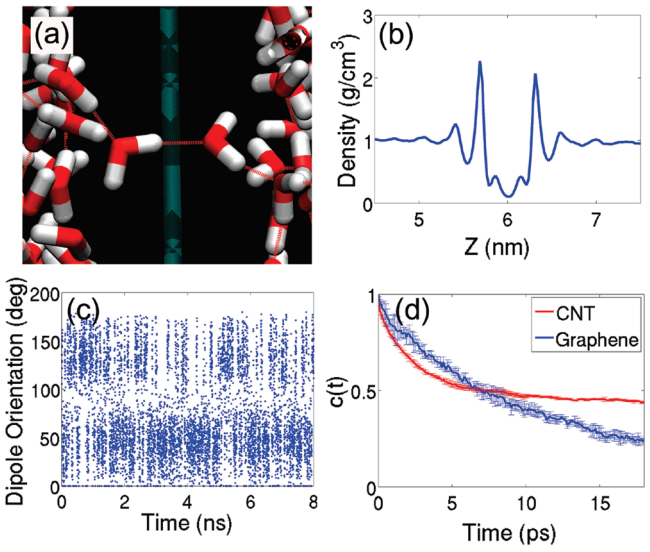

Figure 3. (a) Snap-shot of single-file water configuration across the smaller diameter graphene nanopore. (b) Density distribution of water molecules. Favorable water positions forming single-file structure are indicated as concentration peaks near the graphene membrane. (c) Dipole orientation of single-file water molecules. Density distribution and dipole orientation of single-file structure in CNT are shown in the Supporting Information. (d) Hydrogen-bond autocorrelation function of single-file water molecules in graphene and CNT.

thickness. In the smaller diameter case, water flux in the graphene membrane is lower, while in the larger diameter case, water flux in the graphene membrane is higher compared to that of the CNT membrane. These results indicate that pore diameter is critical in determining whether graphene membrane can transport higher flux compared to the CNT membrane. Since the pore diameter is slightly different in CNT and graphene membranes, a one-atom-thick CNT membrane, containing only one CNT rim, was also tested. The water flux in the (10,0) CNT with one-atom thickness (13.4 ± 1.2 ns^{-1}) is lower compared to the finite thickness (10,0) CNT (16.1 ± 1.9 ns^{-1}). Similarly, the water flux in the (20,20) CNT with one-atom thickness (2790.44 ± 87.12 ns^{-1}) is higher compared to the finite thickness (20,20) CNT (2535 ± 49.82 ns^{-1}). We also tested pores of different diameters ranging from 0.75 to 2.75 nm and found that the water flux is lower in the graphene membrane only in the case of 0.75 nm, where single file water structure was observed. In all other cases, water flux in the graphene membrane is higher compared to the CNT membrane.

In the 0.78 nm diameter CNT membrane, water molecules form single file,[8] and are transported by a hopping mechanism.[26] The water binding sites form a single file structure, and, with increased length of the CNT, the number of water binding sites, N, is also increased. Regardless of the number of water binding sites, N, in the case of a single-file structure, the water flux is invariant.[12,27] In the case of a graphene membrane, water molecules also formed a single file structure with two binding sites (see Figure 3a). The binding sites are shown by two concentration peaks near the graphene membrane, between bulk water and graphene (see Figure 3b). Note that such

DOI: 10.1021/jz100240r | J. Phys. Chem. Lett. 2010, 1, 1590–1594

concentration peaks (the two small peaks just outside the membrane) are not observed in the case of CNT. Although the water transport mechanism is single-file in both cases, the water flux is lower in the graphene membrane, and this is investigated in more detail below.

For single-file water transport, dipole orientation and hydrogen-bonding network play an important role. We calculated the dipole orientation of water molecules that formed the single file chain in the membrane. Dipole orientation is defined as the angle between the water dipole vector and the tube axis and is averaged over all the water molecules in the membrane. In the CNT membrane case, the dipole orientation is either 34° or 146° with a small deviation, and this is maintained over a time period of a few nanoseconds (see Supporting Information). However, the dipole orientation flipped frequently in the graphene membrane, as shown in Figure 3c. This high flipping frequency of the dipole orientation indicates that the hydrogen-bonding breaks frequently. In the case of the CNT membrane, a dipole orientation of 90°, also referred to as the *L* defect or *D* defect,[28] is rarely found. However, a dipole orientation of 90° is frequently observed in the graphene membrane. The presence of defects (or 90° dipole orientation) has been shown to slow down water transport since it requires water reorientation.[28,29]

For a more detailed understanding of hydrogen-bonding dynamics, we calculated the hydrogen-bonding autocorrelation function (HBACF), $c(t)$, of water molecules forming the single-file chain (see Figure 3d). $c(t)$ is the probability of hydrogen-bonded water molecules at time 0 to be hydrogen-bonded at time t. Thus, $c(t)$ measures how fast hydrogen-bonding is relaxed. The faster decrease of $c(t)$ in the graphene membrane suggests that the hydrogen-bonding is relatively weak and breaks frequently. Thus, frequent breaking of hydrogen-bonding combined with the 90° (or defect-like) water dipole orientation contributes to low water transport through the graphene membrane. Even though we applied a pressure drop of 100 MPa, water configuration, including single-file formation and the hydrogen bonding dynamics in equilibrium, is not significantly different from what is reported here.

Negligible variation of water flux with CNT length in small diameter CNT is reported by other researchers,[12,27] and it is attributed to the confinement of water molecules. In the larger 2.71 nm diameter CNT investigated here, we observed that the variation of water flux with length is still negligible. To understand the transport behavior in a larger diameter pore, we calculated the pressure distribution using the Irving−Kirkwood stress tensor (see the Supporting Information for details), and the variation of pressure along the length of the membrane is shown in Figure 4a. The pressure difference between the two bulk regions matches well with the target pressure difference of ΔP = 100 MPa. Even though the pressure difference matched well in all the simulation cases, the absolute value of the pressure was slightly different in each case. These values were adjusted to match at the inlet bulk region for comparison purposes, as shown in Figure 4a. In contrast to continuum hydrodynamics, where the pressure drops linearly along the pore, most of the pressure dropped in the inlet and outlet regions, and the pressure drop inside the

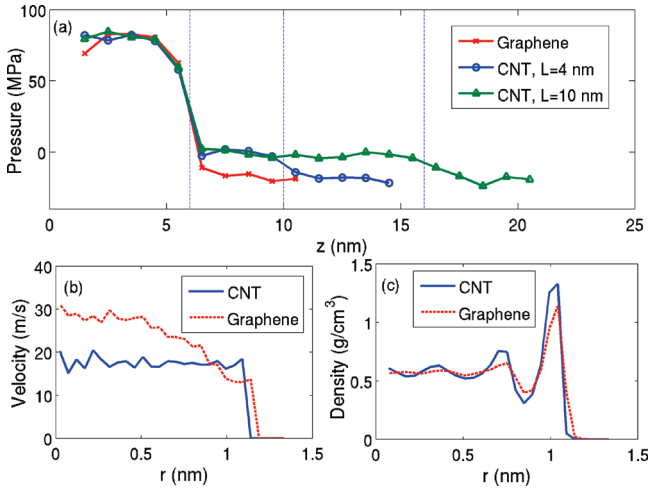

Figure 4. (a) Pressure distribution in a graphene membrane (d = 2.75 nm) and a (20,20) CNT membrane with two different lengths of 4 and 10 nm. Dashed line indicates the position of graphene and the inlet/outlet of the CNT membrane. (b) Axial velocity along the radial direction in the pore. For the CNT, the velocity profile is measured in the middle region of the CNT at z = 11 nm. (c) Radial density distribution of water in a CNT and graphene nanopore. r = 0 denotes the center of the nanopore. In the case of the graphene nanopore, the length of the cylindrical region (in which density is averaged) is defined by the carbon atom diameter.

pore was negligible. Only about 1−4% pressure drop was observed inside the membrane. This is unique to the transport behavior of water through a finite-length CNT, as Huang et al. observed linear pressure variation for liquid argon flow through an artificial nanopore.[30] Our results confirmed the linear pressure variation with liquid argon. We also observed linear pressure variation for water transport through an infinite nanotube (without entrance and exit regions).

Negligible variation of pressure inside the CNT suggests that frictional force is negligible, and the entrance effect is dominant. This explains the insignificant effect of CNT membrane thickness on the water flux. This is different from the theoretical description such as Hagen−Poiseuille (HP) equation derived with linear pressure drop across the tube. The smoothness of the CNT surface and weak CNT−water interaction, namely hydrophobic interaction, can contribute to negligible friction of CNT surface due to the free "OH" bond found in the depletion layer.[9] It should be noted that water flux can depend on the length of the membrane in thicker membranes where entrance effect is not dominant.[31]

The pressure distribution computed above supports the hypothesis that water molecules in thin CNT membranes are transported by collective diffusion[32] rather than viscous flow. The axial velocity profile in the radial direction also supports this transport mechanism. In the center region of the CNT, the velocity distribution is found to be flat (see Figure 4b). In the case of the graphene membrane, inlet and outlet regions overlap. Therefore, the pressure drop appears as a single pressure drop across the membrane. The velocity profile in the graphene membrane was more parabolic with higher velocity at the center. Even though the water velocity away from the center region (near the wall) is smaller than that in the CNT, its contribution to mass flux is also small because of

DOI: 10.1021/jz100240r | *J. Phys. Chem. Lett.* **2010**, *1*, 1590–1594

the low density in that region. Thus, higher water flux in the graphene membrane can be attributed to the higher velocity in the center region of the graphene membrane.

We also investigated the water transport through graphene by computing the energetics of water permeation. It is well-known that the entrance effect plays an important role in water transport through CNT.[10] The energy barrier at the entrance can be estimated by computing the potential of mean force (PMF) of water (see Supporting Information for method). From our equilibrium PMF calculation, representing the potential energy surface along the pore axis, we observed that the energy barrier is dominant at the CNT mouth, and no significant energy barrier was found inside the CNT membrane. The energy barrier for the graphene membrane was lower than that of the CNT membrane (0.32 kT for graphene and 0.423 kT for CNT), suggesting that the water molecules more easily enter the graphene membrane. Since the energy barrier comes from reduced interaction energies, directly connected water baths can be the source of a lower energy barrier in the graphene membrane by creating a more bulk-like environment. In the results shown here, we have considered CNT membranes with thickness/length varying from 2 to 10 nm in 2 nm increments. Systematically decreasing the length/thickness of the CNT membrane to the subnanometer scale can provide additional physical insights, and we will report them in future studies. It is also important to note that pores in other single atom thick membranes (other than a graphene membrane) will likely give similar results to those reported here for graphene.

To conclude, we investigated water transport through a porous graphene membrane and compared it to water transport through thin CNT membranes. For smaller diameter membranes, where single-file structure is observed, water flux is lower through the graphene membrane compared to that of the CNT membrane, primarily due to the frequent rupture of hydrogen bonding network and L/D defect-like water orientation in the graphene pore. On the other hand, for larger diameter pores, where the single-file structure is no longer observed, water flux is higher through the graphene membrane, compared to that of the CNT membrane, as a result of the more bulk-like water neighbors and reduced permeation energy barrier at the entrance. Water flux through the CNT membrane does not vary significantly with different lengths (or thicknesses) for both single-file and non-single-file water structure. This result has been explained by the pressure distribution and plug-like velocity distribution in the pore. Finally, our results indicate that a graphene membrane can be used as an ultra efficient water transporter, compared to thin CNT membranes, whenever the diameter is larger than 0.8 nm.

METHODS

Molecular dynamics simulation was performed using Gromacs 3.3.1.[33] Temperature was maintained at 300 K by using a Nosé−Hoover thermostat with a time constant of 0.1 ps. A periodic boundary condition was applied in all three directions. A simple point charge-extended (SPC/E) model was used for water. Lennard-Jones parameters for carbon atoms were σ = 0.339 nm and ε = 0.2897 kJ/mol.[34] The total number of water molecules varied from 6479 to 14974, depending on the system size. Carbon atoms were frozen to their lattice position to prevent out-of-plane displacement. The simulation box size in the z direction was allowed to fluctuate for 500 ps to adjust the pressure at 1 bar and then switched to the NVT ensemble and run for 1 ns to attain equilibrium. In all cases, equilibrium density of bulk water reservoir was around 1 g/cm^3. After equilibration, the simulation was run for an additional 10−20 ns, depending on the pore diameter, with applied pressure drop, using the methods described below.

When water molecules are within a designated region (shaded region in Figure 1b), external forces are applied on the oxygen atoms of the water molecules to create a pressure drop across the membrane.[35] Applied force on an individual water molecule is given by $f = \Delta PA/n$, where ΔP is the desired pressure drop, A is the area of the membrane, and n is the total number of water molecules in the designated region. Many authors used this method for pressure-driven flow.[11,24,36,37] However, this method should be used with care in order to obtain the desired pressure drop since it is valid if the designated region is in the stationary state. From the local pressure calculation, we validated this method by obtaining the desired pressure drop in the case where enough molecules are within the designated region and the streaming velocity in that region is close to zero. Other methods for pressure-driven flow are also available for a nonperiodic system[30] or a periodic system.[38]

SUPPORTING INFORMATION AVAILABLE Density distribution and dipole orientation of single-file water in a CNT, calculation of hydrogen-bond autocorrelation function, PMF calculation, and calculation of local pressure using the Irving−Kirkwood stress tensor. This material is available free of charge via the Internet at http://pubs.acs.org.

AUTHOR INFORMATION

Corresponding Author:

*To whom correspondence should be addressed. E-mail: aluru@illinois.edu; web address: http://www.illinois.edu/~aluru/.

ACKNOWLEDGMENT This research was supported by the NSF under Grants 0120978 (the Water CAMPWS Center), 0328162 (the nano-CEMMS Center), 0810294, 0852657, and 0915718.

REFERENCES

(1) Shannon, M. A.; Bohn, P. W.; Elimelech, M.; Georgiadis, J. G.; Marinãs, B. J.; Mayes, A. M. Science and Technology for Water Purification in the Coming Decades. *Nature* **2008,** *452*, 301–310.
(2) Hillie, T.; Hlophe, M. Nanotechnology and the Challenge of Clean Water. *Nat. Nanotechnol.* **2007,** *2*, 663–664.
(3) Hinds, B. J.; Chopra, N.; Rantell, T.; Andrews, R.; Gavalas, V.; Bachas, L. G. Aligned Multiwalled Carbon Nanotube Membranes. *Science* **2004,** *303*, 62–65.
(4) Holt, J. K.; Park, H. G.; Wang, Y.; Stadermann, M.; Artyukhin, A. B.; Grigoropoulos, C. P.; Noy, A.; Bakajin, O. Fast Mass

DOI: 10.1021/jz100240r | *J. Phys. Chem. Lett.* **2010,** *1*, 1590–1594

Transport through Sub-2-Nanometer Carbon Nanotubes. *Science* **2006,** *312*, 1034–1037.
(5) Majumder, M.; Chopra, N.; Andrews, R.; Hinds, B. J. Nanoscale Hydrodynamics Enhanced Flow in Carbon Nanotubes. *Nature* **2005,** *438*, 44.
(6) Kumar, M.; Grzelakowski, M.; Zilles, J.; Clark, M.; Meier, W. Highly Permeable Polymeric Membranes Based on the Incorporation of the Functional Water Channel Protein Aquaporin Z. *Proc. Natl. Acad. Sci. U.S.A.* **2007,** *104*, 20719–20724.
(7) Suk, M. E.; Aluru, N. R. Effect of Induced Electric Field on Single-File Reverse Osmosis. *Phys. Chem. Chem. Phys.* **2009,** *11*, 8614–8619.
(8) Hummer, G.; Rasaiah, J. C.; Noworyta, J. P. Water Conduction through the Hydrophobic Channel of a Carbon Nanotube. *Nature* **2001,** *414*, 188–190.
(9) Joseph, S.; Aluru, N. R. Why Are Carbon Nanotubes Fast Transporters of Water? *Nano Lett.* **2008**, *8*, 452−458.
(10) Suk, M. E.; Raghunathan, A. V.; Aluru, N. R. Fast Reverse Osmosis Using Boron Nitride and Carbon Nanotubes. *Appl. Phys. Lett.* **2008,** *92*, 133120.
(11) Corry, B. Designing Carbon Nanotube Membranes for Efficient Water Desalination. *J. Phys. Chem. B* **2008,** *112*, 1427–1434.
(12) Kalra, A.; Garde, S.; Hummer, G. Osmotic Water Transport through Carbon Nanotube Membranes. *Proc. Natl. Acad. Sci. U.S.A.* **2003,** *100*, 10175–10180.
(13) Fornasiero, F.; Park, H. G.; Holt, J. K.; Stadermann, M.; Grigoropoulos, C. P.; Noy, A.; Bakajin, O. Ion Exclusion by Sub-2-nm Carbon Nanotube Pores. *Proc. Natl. Acad. Sci. U.S. A.* **2008,** *105*, 17250.
(14) Striemer, C. C.; Gaborski, T. R.; McGrath, J. L.; Fauchet, P. M. Charge- and Size-Based Separation of Macromolecules Using Ultrathin Silicon Membranes. *Nature* **2007,** *445*, 749–753.
(15) Yamaguchi, A.; Uejo, F.; Yoda, T.; Uchida, T.; Tanamura, Y.; Yamashita, T.; Teramae, N. Self-Assembly of a Silica−Surfactant Nanocomposite in a Porous Alumina Membrane. *Nat. Mater.* **2004,** *3*, 337–341.
(16) Geim, A. K. Graphene: Status and Prospects. *Science* **2009,** *324*, 1530–1534.
(17) Zhao, H.; Min, K.; Aluru, N. R. Size and Chirality Dependent Elastic Properties of Graphene Nanoribbons under Uniaxial Tension. *Nano Lett.* **2009,** *9*, 3012–3015.
(18) Booth, T. J.; Blake, P.; Nair, R. R.; Jiang, D.; Hill, E. W.; Bangert, U.; Bleloch, A.; Gass, M.; Novoselov, K. S.; Katsnelson, M. I. Macroscopic Graphene Membranes and Their Extraordinary Stiffness. *Nano Lett.* **2008,** *8*, 2442–2446.
(19) Hashimoto, A.; Suenaga, K.; Gloter, A.; Urita, K.; Iijima, S. Direct Evidence for Atomic Defects in Graphene Layers. *Nature* **2004,** *430*, 870–873.
(20) Girit, C. O.; Meyer, J. C.; Erni, R.; Rossell, M. D.; Kisielowski, C.; Yang, L.; Park, C. H.; Crommie, M. F.; Cohen, M. L.; Louie, S. G. Graphene at the Edge: Stability and Dynamics. *Science* **2009,** *323*, 1705–1708.
(21) Fischbein, M. D.; Drndi, M. Electron Beam Nanosculpting of Suspended Graphene Sheets. *Appl. Phys. Lett.* **2008,** *93*, 113107.
(22) Sint, K.; Wang, B.; Král, P. Selective Ion Passage through Functionalized Graphene Nanopores. *J. Am. Chem. Soc.* **2008,** *130*, 16448–16449.
(23) Jiang, D.; Cooper, V. R.; Dai, S. Porous Graphene as the Ultimate Membrane for Gas Separation. *Nano Lett.* **2009,** *9*, 4019–4024.
(24) Gong, X.; Li, J.; Lu, H.; Wan, R.; Li, J.; Hu, J.; Fang, H. A Charge-Driven Molecular Water Pump. *Nat. Nanotechnol.* **2007,** *2*, 709–712.
(25) Bunch, J. S.; Verbridge, S. S.; Alden, J. S.; van der Zande, A. M.; Parpia, J. M.; Craighead, H. G.; McEuen, P. L. Impermeable Atomic Membranes from Graphene Sheets. *Nano Lett.* **2008,** *8*, 2458–2462.
(26) Berezhkovskii, A.; Hummer, G. Single-File Transport of Water Molecules through a Carbon Nanotube. *Phys. Rev. Lett.* **2002,** *89*, 64503.
(27) Portella, G.; Pohl, P.; de Groot, B. L. Invariance of Single-File Water Mobility in Gramicidin-like Peptidic Pores as a Function of Pore Length. *Biophys. J.* **2007,** *92*, 3930–3937.
(28) Dellago, C.; Naor, M. M.; Hummer, G. Proton Transport through Water-Filled Carbon Nanotubes. *Phys. Rev. Lett.* **2003,** *90*, 105902.
(29) Won, C. Y.; Joseph, S.; Aluru, N. R. Effect of Quantum Partial Charges on the Structure and Dynamics of Water in Single-Walled Carbon Nanotubes. *J. Chem. Phys.* **2006,** *125*, 114701.
(30) Huang, C.; Nandakumar, K.; Choi, P. Y. K.; Kostiuk, L. W. Molecular Dynamics Simulation of a Pressure-Driven Liquid Transport Process in a Cylindrical Nanopore Using Two Self-Adjusting Plates. *J. Chem. Phys.* **2006,** *124*, 234701.
(31) Peng, X.; Jin, J.; Nakamura, Y.; Ohno, T.; Ichinose, I. Ultrafast Permeation of Water through Protein-Based Membranes. *Nat. Nanotechnol.* **2009,** *4*, 353–357.
(32) Zhu, F.; Tajkhorshid, E.; Schulten, K. Collective Diffusion Model for Water Permeation through Microscopic Channels. *Phys. Rev. Lett.* **2004,** *93*, 224501.
(33) Van Der Spoel, D.; Lindahl, E.; Hess, B.; Groenhof, G.; Mark, A. E.; Berendsen, H. J. C. GROMACS: Fast, Flexible, and Free. *J. Comput. Chem.* **2005,** *26*, 1701–1708.
(34) Chen, G.; Guo, Y.; Karasawa, N.; Goddard, W. A., III Electron−Phonon Interactions and Superconductivity in K_3C_{60}. *Phys. Rev. B* **1993,** *48*, 13959–13970.
(35) Zhu, F.; Tajkhorshid, E.; Schulten, K. Pressure-Induced Water Transport in Membrane Channels Studied by Molecular Dynamics. *Biophys. J.* **2002,** *83*, 154–160.
(36) Li, J.; Gong, X.; Lu, H.; Li, D.; Fang, H.; Zhou, R. Electrostatic Gating of a Nanometer Water Channel. *Proc. Natl. Acad. Sci. U.S.A.* **2007,** *104*, 3687–3692.
(37) Goldsmith, J.; Martens, C. C. Pressure-Induced Water Flow through Model Nanopores. *Phys. Chem. Chem. Phys.* **2009,** *11*, 528–533.
(38) Li, J.; Liao, D.; Yip, S. Coupling Continuum to Molecular-Dynamics Simulation: Reflecting Particle Method and the Field Estimator. *Phys. Rev. E* **1998,** *57*, 7259.

DOI: 10.1021/jz100240r | *J. Phys. Chem. Lett.* **2010,** *1*, 1590–1594